ACS Medicinal Chemistry Letters

Letter

Structure-Based Discovery of Phenyl (3-Phenylpyrrolidin-3-yl)sulfones as Selective, Orally Active ROR#t Inverse Agonists

James J.-W. Duan, Zhonghui Lu, Bin jiang, Sylwia Stachura, Carolyn A. Weigelt, John S. Sack, Javed Khan, Max Ruzanov, Michael A. Galella, Dauh-Rurng Wu, Melissa Yarde, Ding Ren Shen, David J. Shuster, Virna Borowski, Jenny H. Xie, Lisa Zhang, Sridhar Vanteru, Arun Kumar Gupta, Arvind Mathur, Qihong Zhao, William Foster, Luisa M. Salter-Cid, Percy H Carter, and T. G. Murali Dhar

ACS Med. Chem. Lett., **Just Accepted Manuscript** • DOI: 10.1021/acsmedchemlett.9b00010 • Publication Date (Web): 26 Feb 2019

ACS Publications

is published by the American Chemical Society. 1155 Sixteenth Street N.W., Washington, DC 20036

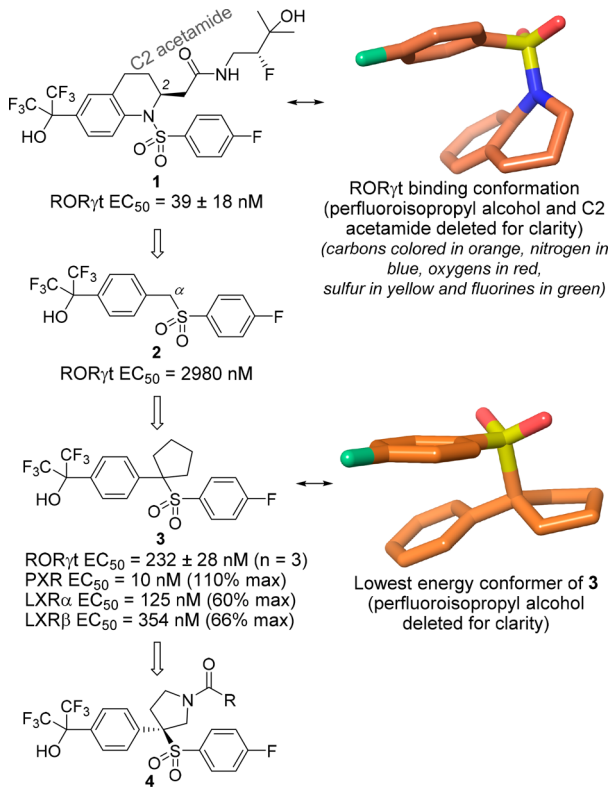

Figure 1. Previously reported sulfonamide **1** and newly designed benzylsulfone **2**, (1-phenylcyclopentyl)sulfone **3**, and (3-phenylpyrrolidin-3-yl)sulfone **4**.

bound to RORγt, was that the sulfonyl group adopted a pseudoaxial orientation with respect to the THQ core, and the *para*-fluorophenyl group was stacked against the phenyl ring of the THQ in a face-to-face fashion, resulting in an overall near U-shaped conformation (3-D picture in Figure 1). While searching for alternative scaffolds, we noticed that phenyl benzylsulfones have been reported to prefer a conformation reminiscent of the binding mode of **1**.[10,11] Therefore, we set out to explore a series of phenyl benzylsulfones as alternatives to the THQ sulfonamide core.[12,13]

To quickly assess the impact on activity, the parent phenyl benzylsulfone **2** (Figure 1) was selected as the initial target. In a RORγt inverse agonist assay (a Gal-4 reporter assay using the Jurkat cell line),[9] compound **2** exhibited an EC_{50} of 2980 nM. We envisioned that α,α-disubstitution at the benzyl position would enhance the population of the U-shaped conformation, through the Thorpe−Ingold effect, and in turn improve potency. After exploring different substituents *in silico*, phenyl (1-phenylcyclopentyl)sulfone **3** (predicted the lowest energy conformation shown in Figure 1) was selected as the target to synthesize. To our delight, this benzylic methylene-to-cyclopentane transformation increased RORγt potency by more than 10-fold (232 nM for **3** vs 2980 nM for **2**). Unfortunately, compound **3** displayed significant cross reactivity against PXR and liver X receptor α and β (LXRα and LXRβ). We had reported earlier that in the THQ series, the C2 acetamide group of **1** played an important role in significantly right shifting PXR, LXRα, and LXRβ potency,[9] so it was logical to explore the acetamide binding site in order to improve selectivity of the sulfone series (**3**). With this in mind, phenyl (3-phenylpyrrolidin-3-yl)sulfone **4** was designed. Molecular modeling studies of **4** with the ligand-binding domain (LBD) of RORγt suggested that the acyl substituents off the pyrrolidine nitrogen (−COR in **4**) could provide a suitable vector toward the C2 acetamide site. An added benefit of the cyclopentane-to-pyrrolidine switch was that the pyrrolidine ring would allow rapid structure−activity relationship (SAR) study through simple acylation reactions.

The free NH pyrrolidine **5** (*R*-enantiomer, Table 1) was 2.5-fold less potent against RORγt than the cyclopentane **3**. Small amide, carbamate, and urea analogues **6**−**8** (all racemic mixtures) resulted in slightly weaker activity than **5**, while the larger cyclopentylcarboxamide **9** (racemic mixture) restored potency to the level of **3**. Noteworthy here is that pyrrolidines **5**−**9** displayed weaker activities against PXR, LXRα, and LXRβ compared to **3**.

Table 1. Initial Pyrrolidinylsulfone Analogues

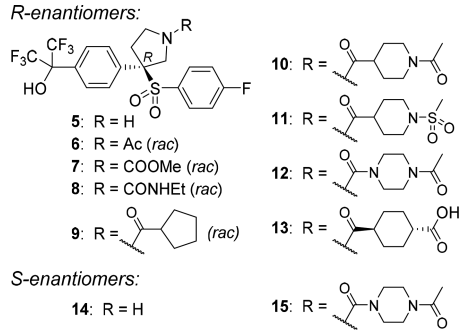

#	RORγt EC_{50} nM[a]	PXR EC_{50} nM[b] (% max)[c]	LXRα[d] EC_{50} nM[b] (% max)	LXRβ[d] EC_{50} nM[b] (% max)
5	595 ± 237	434 (110)	2920 (58)	>7500
6	2650 ± 1280	480 (100)	>7500	>7500
7	1040[b]	ND	408 (62)	1900 (39)
8	1260[b]	ND	>7500	>7500
9	378 ± 224	794 (99)	>7500	>7500
10	224 ± 78	7810 (81)	>7500	>7500
11	88 ± 35	>2470 (89)	>7500	>7500
12	55 ± 25	4930 (86)	>7500	>7500
13	4340 ± 847	>50000 (11)	>3750	>7500
14	4500 ± 1750	520 (110)	>7500	>7500
15	4200[b]	>5140 (72)	>7500	>7500

[a]RORγt reporter assay using a Jurkat cell line; values from two or more experiments performed in duplicate unless otherwise noted; % max typically close to 100%. [b]Value from a single experiment performed in duplicate. [c]% max relative to rifampicin. [d]LXR assays (agonist mode) were performed using a CV-1 cell line; % max relative to T0901317. ND = not determined.

Examination of the RORγt cocrystal structure with an analogue of **1** (compound **33** in ref 9) revealed that the *tert*-alcohol of the C2 acetamide group is surrounded by polar side chains comprising Arg364, Arg367, and Tyr281 as well as the carbonyl group of Cys285. To engage these amino acids, a biased SAR effort to incorporate polar amide groups was carried out (analogues **10**−**13**, *R* enantiomer, Table 1). Compared to the cyclopentane **3**, compounds **10**−**12** showed comparable or better potency against RORγt. Importantly, **10**−**12** completely dialed out LXRα and LXRβ activities (>7.5 μM). Their PXR EC_{50} values were also significantly right-shifted (greater than 100-fold) compared to **3**, although Y_{max} values were still high. Carboxylic acid **13** was less active. Analogues incorporating the *S*-pyrrolidine enantiomer were also evaluated. Compounds **14** and **15**, the corresponding *S*-

DOI: 10.1021/acsmedchemlett.9b00010
ACS Med. Chem. Lett. XXXX, XXX, XXX−XXX

enantiomers of **5** and **12** respectively, were considerably weaker against RORγt.

In order to validate the hypothesis regarding the binding conformation of phenyl (3-phenylpyrrolidin-3-yl)sulfones and the proposed engagement of key amino acid residues in the polar pocket, an X-ray structure of **12** with the RORγt LBD was obtained (Figure 2). As predicted from modeling, the

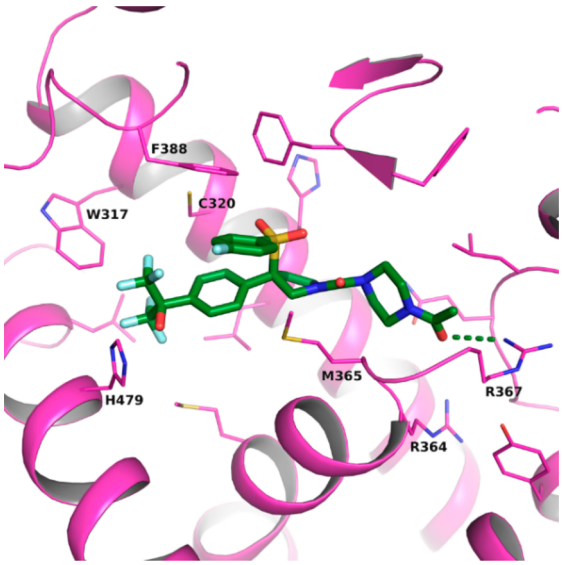

Figure 2. X-ray crystal structure of compound **12** and the LBD of RORγt (PDB ID 6NXH). The carbons of the protein are colored in pink and those of **12** in green. Sulfurs are colored in yellow, N in blue, O in red and F in cyan. A hydrogen bond of **12** with Arg367 of RORγt is indicated by a dashed line.

benzyl phenyl sulfone backbone of **12** adopted a near U-shaped conformation and interacts with RORγt in a fashion reminiscent of the bicyclic sulfonamide series (**1**). Specifically, the *p*-fluorophenyl group occupies a hydrophobic pocket formed by the side chains of Met365, Val376, Phe378, Phe388, Ile400, and Phe401 (not shown for clarity except Phe388 and Met365) and forms a face-to-face π stacking interaction with the side chain of Phe388. The two CF_3 substituents of the hexafluoroisopropanol group also occupy a hydrophobic pocket, formed by the side chains of residues Trp317, Met358, Leu391, Ile397, Ile400, and His479 (some not shown in Figure 2 for clarity). Although the hydroxy group is in the vicinity of His479 on helix 11, it does not appear to have the desired orientation to form a hydrogen bond. The implications of this will become apparent in subsequent SAR studies (*vide infra*). In the center of the RORγt pocket, the pyrrolidine ring makes hydrophobic contacts with the side chains of Leu324, Met365, and Val361. The pyrrolidine moiety also provides a vector for the 4-acylpiperazinylcarbonyl substituent to bind in the polar acetamide binding pocket. Consistent with our hypothesis, the 4-acyl group forms a hydrogen bond with the side chain of Arg367.

A crystal structure of **3** in the PXR LBD was also solved. Interestingly, **3** binds to PXR in two binding modes that differ in the orientation of the *p*-fluorophenylsulfonyl group and the benzene linker between the cyclopentane and the hexafluoroisopropyl alcohol (Figure 3). The hexafluoroisopropyl alcohol group is positioned in the same fashion in both binding modes: with the hydroxy group forming a hydrogen bond to the side

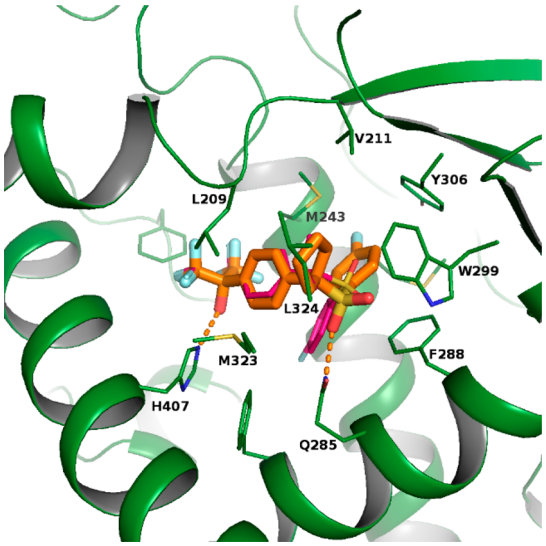

Figure 3. X-ray crystal structure of compound **3** and the LBD of PXR (PDB ID 6NX1). Compound **3** binds to PXR in alternate conformations with 70%/30% occupancy, as depicted by thicker sticks (orange) and skinnier sticks (magenta), respectively. The carbons of the protein are colored in green. Sulfurs are colored in yellow, N in blue, O in red, and F in cyan. Hydrogen bonds of **3** with PXR are indicated by dashed lines.

chain of His407 and the trifluoromethyl groups fill a small hydrophobic pocket. In both binding modes, the cyclopentane ring projects into an enclosed hydrophobic pocket formed by the side chains of Leu209, Val211, Trp299, Leu308, Met323, and Leu324. This structure could explain the reduced PXR potency of **10**−**12**. The substituted pyrrolidines in **10**−**12** would be too polar and sterically encumbered to fit in the small hydrophobic pocket. As a result, analogues **10**−**12** exhibited improved selectivity against PXR compared to **3**.

Using the cyclopentyl sulfone **3** as a starting point, SAR around the hexafluoroisopropyl alcohol moiety was investigated (Table 2). Incorporating a methyl group in place of one of the CF_3 resulted in 6-fold loss of RORγt potency (**16**, racemic mixture). The corresponding ethyl analogue **17** (racemic mixture) partially restored activity. Attempts to

Table 2. Hexafluoroisopropyl Alcohol SAR

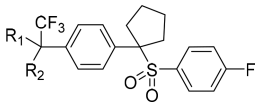

#	R_1	R_2	RORγt EC_{50} nM[a]	PXR EC_{50} nM[b] (% max)[c]
3	CF_3	OH	232 ± 28	10 (110)
16[d]	Me	OH	1400 ± 390	239 (110)
17[d]	Et	OH	643[b]	48 (110)
18	CF_3	NH_2	888 ± 573	275 (120)
19	CF_3	OMe	1130 ± 65	920 (110)
20	CF_3	Me	3650[b]	752 (140)
21	CF_3	F	494[b]	1010 (130)
22	CF_3	Cl	271 ± 337	229 (110)

[a]RORγt reporter assay using a Jurkat cell line; values from two or more experiments performed in duplicate unless otherwise noted; % max typically close to 100%. [b]Value from a single experiment performed in duplicate. [c]% max relative to rifampicin. [d]Tested as racemic mixture.

DOI: 10.1021/acsmedchemlett.9b00010
ACS Med. Chem. Lett. XXXX, XXX, XXX−XXX

Table 3. *In Vitro* Profile of Perfluoroisopropyl Analogues[a]

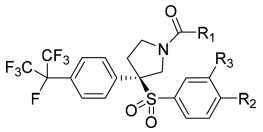

#	R_1	R_2	R_3	RORγt EC_{50} nM[b]	PXR EC_{50} nM[c] (% max.)[d]	MLM (% remaining)[e]	hPB, mPB (% unbound)
23	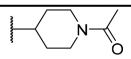	F	H	269 ± 6	>50000 (7)	ND	ND
24	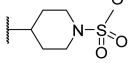	F	H	161 ± 51	>50000 (2)	69	ND
25	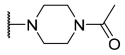	F	H	48 ± 38	>50000 (10)	68	ND
26	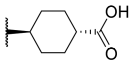	F	H	119 ± 28	>50000 (18)	86	3.7, 10.5
27	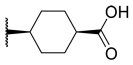	F	H	4230[c]	ND	ND	ND
28	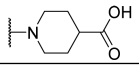	F	H	383 ± 102	>46100 (23)	88	ND
29	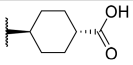	H	H	396 ± 61	>50000 (10)	96	ND
30	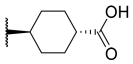	Me	H	64 ± 5	12600 (29)	85	1.3, 2.6
31	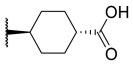	Et	H	84 ± 61	>50000 (3)	100	ND
32	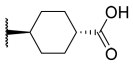	Cl	H	106 ± 39	6440 (22)	100	ND
33	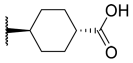	OMe	H	686[c]	>50000 (12)	98	ND
34	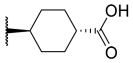	F	Me	61 ± 20	>22800 (40)	84	1.7, 2.9
35	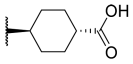	F	Et	54 ± 7	>50000 (9)	73	ND
36	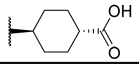	F	*c*-Pr	149[c]	>50000 (9)	74	ND

[a]All compounds showed EC_{50} values greater than 7500 nM in LXRα and LXRβ assays. [b]RORγt reporter assay using a Jurkat cell line; values from two or more experiments performed in duplicate unless otherwise noted; % max typically close to 100%. [c]Value from a single experiment performed in duplicate. [d]% max relative to rifampicin. [e]Metabolic stability in mouse liver microsome; percentage remaining after 10 min of incubation. ND = not determined.

replace the hydroxyl group with an amino, methoxy, methyl, fluoro, or chloro group all led to weaker RORγt inverse agonists (**18**−**22**). Among them, **21** and **22** were found to have potency closest to **3**. The perfluoroisopropyl analogue **21** was especially interesting because it had dramatically right-shifted PXR activity compared to **3** (100-fold), while being only 2-fold less potent at RORγt. The right shift in PXR EC_{50} for analogue **21** can potentially be explained by the X-ray cocrystal structures of compounds **12** and **3** (Figures 2 and 3, respectively). Assuming that **3** binds like **12** in RORγt, the hydroxy group would not be involved in hydrogen bonding and, therefore, can be replaced with a fluoro group (**21**) without significant loss of activity. In PXR, the hydroxy group of **3** serves as a hydrogen bond donor. The fluoro replacement cannot maintain this hydrogen bond. As a result, **21** displayed a dramatic loss of PXR potency.

In order to further improve RORγt potency and selectivity of compound **21** for PXR, SAR of the perfluoroisopropyl moiety in combination with the pyrrolidinylsulfone scaffold was carried out (Table 3). Compounds **23** and **25** showed similar RORγt potency to the corresponding alcohols **10** and **12** (Table 1), while **24** was 2-fold weaker than **11**. Surprisingly, the cyclohexanecarboxylic acid **26** was quite active with an EC_{50} of 119 nM, 35-fold more potent than the corresponding alcohol **13**. The *trans*-cyclohexane stereochemistry in **26** is important as the *cis* isomer **27** was significantly less potent for RORγt. Replacing the cyclohexane with a piperidine moiety also resulted in a less potent compound (**28**).

To gain insight into the potency disconnect, **13** and **26** were tested in a RORγt binding assay. While the binding IC_{50} of **26** (55 nM) correlated reasonably well with its Jurkat activity, **13** displayed considerably more potent binding (146 nM) than its Jurkat IC_{50}. We hypothesized that cell membrane permeability was probably responsible for the poor functional activity of **13** in the Jurkat assay. Consistent with this hypothesis, compound **13** showed low permeability in Caco-2 assay (permeation coefficient less than 15 nm/s). In contrast, analogue **26** showed significantly improved permeability (120 nm/s).

The effect of substituents on the phenylsulfone moiety was also studied (**29**−**36**, Table 3). Replacing the *para*-fluoro

DOI: 10.1021/acsmedchemlett.9b00010
ACS Med. Chem. Lett. XXXX, XXX, XXX−XXX

group (R_2) in **26** with a methyl, ethyl, or chloro group (**30**–**32**) maintained or slightly improved RORγt activity vs **26**, whereas the hydrogen and methoxy analogues (**29** and **33**) led to reduced activity. Additional analogues of **26** with *meta*-substituents (R_3) were also synthesized. Methyl and ethyl analogues (**34** and **35**) improved activity by approximately 2-fold vs **26**. A larger cyclopropyl analogue **36** was slightly less active.

The SAR outlined in Table 3 clearly shows that the perfluoroisopropyl moiety consistently improved selectivity against PXR for the pyrrolidinylsulfone series. All compounds in Table 3 showed PXR Y_{max} under 40%, with most of them having EC_{50} values greater than the assay limit. These compounds also exhibited excellent selectivity against LXRα and LXRβ, typically with EC_{50} values greater than 7.5 μM.

To identify a tool compound for *in vivo* studies, majority of the compounds in Table 3 were first tested in a 10 min mouse liver microsome (MLM) assay to get a rough estimation of microsomal stability. Compounds **24** and **25** were found to have moderate stability (69% and 68% remaining after 10 min incubation). In general, compounds with carboxylic acid moieties showed improved stability in the MLM assay (for example, **26**, **30**, and **34**). Compounds **26**, **30**, and **34** were also tested for protein binding, and **26** was found to have the highest free fraction (3.7% and 10.5% unbound in human and mouse proteins, respectively). Based on its overall profile in terms of RORγt potency, selectivity, metabolic stability, and protein binding, analogue **26** was selected for further evaluation.

Compound **26** was inactive against RORα and RORβ in either inverse agonist or agonist mode (>40 μM). In addition to its selectivity against PXR, LXRα, and LXRβ (*vide supra*), **26** displayed IC_{50} values greater than 150 μM against the broader family of nuclear receptors including androgen receptor, estrogen receptor α, glucocorticoid receptor, and progesterone receptor. Compound **26** was also tested in a panel of 38 additional assays ranging from GPCRs, transporters, enzymes, and ion channels and was found to be inactive within the concentration limit of the assays (typically 30 μM).

In the Caco-2 assay, **26** demonstrated good permeability (Pc of 120 nm/s) with a modest efflux ratio of 2.6. It showed no significant *in vitro* inhibition against a panel of cytochrome P450 isozymes (IC_{50} > 20 μM for 1A2, 1B2, 2C9, 2C19, 2D6, and 3A4), except 2C8 (IC_{50} of 0.68 μM). In a more accurate $t_{1/2}$ MLM assay, **26** displayed a stability half-life of greater than 120 min, which translated into low clearance (7.2 mL/min/kg) and a long half-life (7.2 h) after intravenous administration of 2 mg/kg in mice (Table 4). An oral dose of 10 mg/kg of **26** led to an excellent overall profile with C_{max} of 6.6 μM, AUC (area under the curve) of 36.6 μM·h, and an oral bioavailability of 99%.

Having identified compound **26** as a highly selective RORγt inverse agonist with an excellent mouse PK profile, we tested the compound in an IL-2/IL-23-stimulated mouse pharmacodynamic (PD) model (Figure 4).[9] In the study, naive mice were challenged three times with IL-2 and IL-23 (at 0, 7, and 23 h) after IL-2 alone priming (−24 h), and **26** was dosed orally 30 min prior to each IL-2/IL-23 challenge. Serum was analyzed 7 h after the last IL-2/IL-23 administration. As shown in Figure 4, at oral bid doses of 5, 15, and 50 mg/kg, **26** achieved 47%, 77%, and 98% inhibition of IL-17F production, respectively. In addition, dose-dependent inhibition of IL-17A, IL-22, GM-CSF, KC (mouse IL-8), and IL-6 was also observed (data not shown). Collectively, these data demonstrated that **26** effectively blocked RORγt-dependent cytokine production in mice.

Table 4. Pharmacokinetic Profile of 26 in balb/c Mice[a]

	dose	
	2 mg/kg (iv)	10 mg/kg (po)
C_{max} (μM)		6.6
T_{max} (h)		2
AUC (μM·h)	7.4	36.6
$t_{1/2}$ (h)	7.2	
Cl (mL/min/kg)	7.2	
Vss (L/kg)	3.4	
F (%)		99

[a]Dose vehicle: iv− 2.5% *N*-methyl-2-pyrrolidone, 67.5% polyethylene glycol 300, 4.5% pluronic F-68, 25.5% water; po− 5% *N*-methyl-2-pyrrolidone, 76% polyethylene glycol 300, 19% D-α-tocopheryl polyethylene glycol succinate (TPGS).

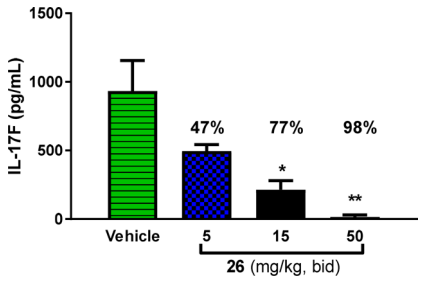

Figure 4. Inhibition of IL-17F production in an IL-2/IL-23 induced mouse PD model after oral administration of **26**.

Compound **26** was also tested in an IL23-induced mouse model of acanthosis (see Supporting Information for description of this model).[14] As illustrated in Figure 5, **26** significantly reduced ear swelling at both 10 and 50 mg/kg when dosed orally, bid. At the 50 mg/kg bid dose, **26** achieved efficacy nearly equivalent to an anti-IL-23 antibody, which was used as the positive control in this model.

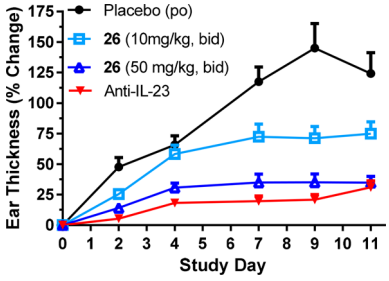

Figure 5. Efficacy of **26** in an IL-23-induced mouse acanthosis model.

Detailed protocols for the synthesis of compounds listed in Tables 1−3 are provided in Supporting Information. Schemes 1 and 2 highlight representative syntheses of cyclopentylsulfones and pyrrolidinylsulfone **26**. The methyl group of commercially available **37** was subjected to radical bromination conditions, and the product mixture (mostly monobromide) was reacted with sodium 4-fluorobenzenesulfinate to provide compound **2** (Scheme 1).[15] After protection of the alcohol as a benzyl ether, the resulting intermediate **38** was treated with sodium hydride and (*Z*)-1,4-dichlorobut-2-ene to give the

DOI: 10.1021/acsmedchemlett.9b00010
ACS Med. Chem. Lett. XXXX, XXX, XXX−XXX

Scheme 1. Synthesis of Cyclopentylsulfone Analogues[a]

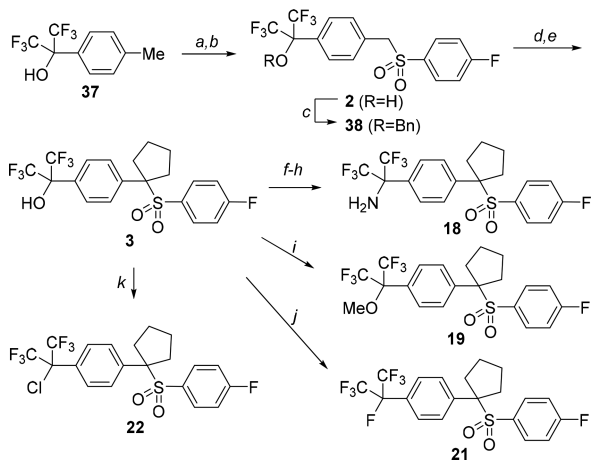

[a]Reagents and conditions: (a) NBS, AIBN, CCl_4, at reflux; (b) sodium 4-fluorobenzenesulfinate, DMF, 82% two steps; (c) BnBr, K_2CO_3, DMF, 87%; (d) (*Z*)-1,4-dichlorobut-2-ene, NaH, DMF, 70%; (e) H_2, $Pd(OH)_2/C$, MeOH, EtOAc, 39%; (f) Tf_2O, KOMe, toluene, 42%; (g) NaN_3, TfOH, 40 °C, 61%; (h) H_2, Pd/C, MeOH, CH_2Cl_2, 99%; (i) MeI, K_2CO_3, DMF, 78%); (j) DAST, CH_2Cl_2, 85 °C, 54%; (k) $SOCl_2$, pyridine, at reflux, 46%.

Scheme 2. Synthesis of Pyrrolidinylsulfone 26[a]

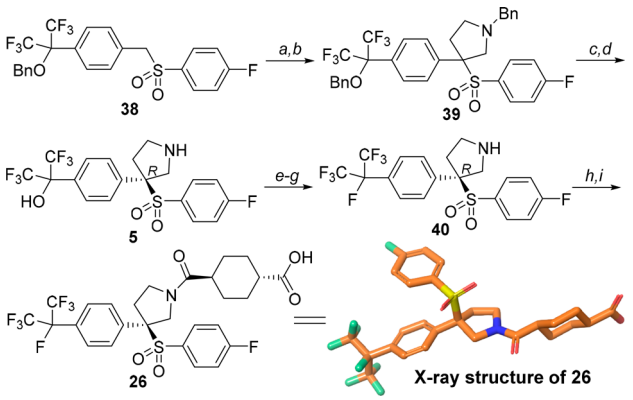

[a]Reagents and conditions: (a) $Me_2NCH_2NMe_2$, Ac_2O, DMF, 60 °C, 55%; (b) *N*-benzyl-1-methoxy-*N*-((trimethylsilyl)methyl)-methanamine, TfOH, CH_2Cl_2, 96%; (c) chiral separation, 43%; (d) H_2, $Pd(OH)_2/C$, HCl, MeOH, 98%; (e) $(Boc)_2O$, *i*-Pr_2NEt, CH_2Cl_2, 96%; (f) DAST, $ClCH_2CH_2Cl$, 50 °C, 77%; (g) HCl, 1,4-dioxane, 99%; (h) *trans*-1,4-cyclohexanedicarboxylic acid monomethyl ester, BOP, *i*-Pr_2NEt, DMF, 98%; (i) LiOH, THF, H_2O, 78%.

cyclopentene product. Reduction of the olefin and cleavage of the benzyl ether in one pot provided **3**, which served as an intermediate for additional analogues. For example, **3** was converted to amine **18** via a three-step sequence: triflate formation, azide displacement, and reduction to amine.[16] Compound **3** was also used to synthesize methyl ether **19**, fluoride **21**, and chloride **22**.[17]

The synthesis of pyrrolidinylsulfone **26** is depicted in Scheme 2. Compound **38** was treated with *N,N,N′,N′*-tetramethylmethylenediamine and acetic anhydride to give a vinyl sulfone,[18] which underwent acid-catalyzed [3 + 2] cycloaddition with *N*-benzyl-1-methoxy-*N*-((trimethylsilyl)-methyl)methanamine to provide pyrrolidine **39**.[19] After resolution of enantiomers using supercritical fluid chromatography (SFC), the desired *R* enantiomer was globally deprotected to give **5**. After Boc protection of the pyrrolidine, the resulting alcohol was treated with DAST followed by HCl to yield **40**. Finally, BOP-mediated coupling with *trans*-1,4-cyclohexanedicarboxylic acid monomethyl ester followed by saponification completed the synthesis of **26**. The structure of **26** was determined by single crystal X-ray analysis (CCDC 1896035).

In summary, a novel series of RORγt inverse agonists was discovered using rational drug design. Cyclopentylsulfone **3** exhibited promising RORγt potency, but lacked selectivity against PXR, LXRα, and LXRβ. Subsequent discovery of the pyrrolidinylsulfone in combination with the perfluoroisopropyl group led to discovery of selective RORγt inverse agonists. Lead compound **26** displayed high selectivity *in vitro* and an excellent pharmacokinetic profile in mouse. When tested *in vivo*, **26** exhibited dose-dependent activity in an IL2/IL23 mouse PD model and achieved biologic-like efficacy in an IL23-induced acanthosis mouse model of psoriasis.

■ ASSOCIATED CONTENT

Supporting Information

The Supporting Information is available free of charge on the ACS Publications website at DOI: 10.1021/acsmedchemlett.9b00010.

Description of acanthosis model and synthesis and characterization of new compounds (PDF)

■ AUTHOR INFORMATION

Corresponding Author

*E-mail james.duan@bms.com. Phone: 609-252-4199.

ORCID

James J.-W. Duan: 0000-0003-2730-9924
Percy H. Carter: 0000-0002-5880-1164
T. G. Murali Dhar: 0000-0003-0738-1021

Notes

The authors declare no competing financial interest.

■ ACKNOWLEDGMENTS

We would like to thank Dr. Robert Borzilleri for critical review of the manuscript.

■ REFERENCES

(1) Cook, D. N.; Kang, H. S.; Jetten, A. M. Retinoic acid-related orphan receptors (RORs): regulatory functions in immunity, development, circadian rhythm, and metabolism. *Nucl. Receptor Res.* **2015**, 101185.

(2) Ivanov, I. I.; McKenzie, B. S.; Zhou, L.; Tadokoro, C. E.; et al. The orphan nuclear receptor RORγt directs the differentiation program of proinflammatory IL-17+ T helper cells. *Cell* **2006**, *126*, 1121.

(3) Balato, A.; Scala, E.; Balato, N.; Caiazzo, G.; et al. Biologics that inhibit the Th17 pathway and related cytokines to treat inflammatory disorders. *Expert Opin. Biol. Ther.* **2017**, *17*, 1363.

(4) Frieder, J.; Kivelevitch, D.; Haugh, I.; Watson, I.; et al. Anti-IL-23 and anti-IL-17 biologic agents for the treatment of immune-mediated inflammatory conditions. *Clin. Pharmacol. Ther.* **2018**, *103*, 88.

(5) Dhar, T. G. M.; Zhao, Q.; Markby, D. W. Targeting the nuclear hormone receptor RORγt for the treatment of autoimmune and inflammatory disorders. *Annu. Rep. Med. Chem.* **2013**, *48*, 169.

(6) Fauber, B. P.; Magnuson, S. Modulators of the nuclear receptor retinoic acid receptor-related orphan receptor-c (RORc or RORc). *J. Med. Chem.* **2014**, *57*, 5871.

DOI: 10.1021/acsmedchemlett.9b00010
ACS Med. Chem. Lett. XXXX, XXX, XXX−XXX

(7) Cyr, P.; Bronner, S. M.; Crawford, J. J. Recent progress on nuclear receptor RORc modulators. *Bioorg. Med. Chem. Lett.* **2016**, *26*, 4387.

(8) Pandya, V. B.; Kumar, S.; Sachchidanand; Sharma, R.; et al. Combating autoimmune diseases with retinoic acid receptor-related orphan receptor-γ (RORγ or RORc) inhibitors: hits and misses. *J. Med. Chem.* **2018**, *61*, 10976.

(9) Gong, H.; Weinstein, D. S.; Lu, Z.; Duan, J. J.-W.; et al. Identification of bicyclic hexafluoroisopropyl alcohol sulfonamides as retinoic acid receptor-related orphan receptor gamma (RORγ/RORc) inverse agonists. Employing structure-based drug design to improve pregnane X receptor (PXR) selectivity. *Bioorg. Med. Chem. Lett.* **2018**, *28*, 85.

(10) Scott, J. P.; Lieberman, D. R.; Beureux, O. M.; Brands, K. M.; et al. A practical synthesis of a γ-secretase inhibitor. *J. Org. Chem.* **2007**, *72*, 4149.

(11) Butler, J. D.; Donald, M. B.; Ding, Z.; Fettinger, J. C.; et al. Phenylsulfonyl as a directing group for nitrile oxide cycloadditions and mCPBA epoxidations. *Tetrahedron Lett.* **2009**, *50*, 5110.

(12) Duan, J.; Dhar, T. G. M.; Jiang, B.; Lu, Z. et al. Carbocyclic sulfone RORγ modulators. US Patent 9,771,320; September 26, 2017.

(13) Duan, J.; Dhar, T. G. M.; Jiang, B.; Lu, Z. et al. Pyrrolidinyl sulfone derivatives and their use as RORγ modulators. U.S. Patent 9,458,171; October 4, 2016.

(14) Rizzo, H. L.; Kagami, S.; Phillips, K. G.; Kurtz, S. E.; et al. IL-23-mediated psoriasis-like epidermal hyperplasia is dependent on IL-17A. *J. Immunol.* **2011**, *186*, 1495.

(15) Becker, D. P.; DeCrescenzo, G. A.; Malecha, J. W.; Miyashiro, J. M. et al. Preparation of sulfone liver X-receptor modulators. US Patent 6,822,120; November 23, 2004.

(16) Nesi, M.; Brasca, M. G.; Longo, A.; Moretti, W.; et al. Generation of doubly trifluoromethyl substituted carbocations: synthesis of α,α-bis(trifluoromethyl)benzylamines. *Tetrahedron Lett.* **1997**, *38*, 4881.

(17) Reynolds, D. W.; Cassidy, P. E.; Johnson, C. G.; Cameron, M. L. Exploring the chemistry of the 2-arylhexafluoro-2-propanol group: synthesis and reactions of a new highly fluorinated monomer intermediate and its derivatives. *J. Org. Chem.* **1990**, *55*, 4448.

(18) Scott, J. P.; Hammond, D. C.; Beck, E. M.; Brands, K. M. J.; et al. Expedient Diels-Alder assembly of 4-aryl-4-phenylsulfonylcyclohexanones. *Tetrahedron Lett.* **2004**, *45*, 3345.

(19) Terao, Y.; Kotaki, H.; Imai, N.; Achiwa, K. Trifluoroacetic acid-catalyzed 1,3-cycloaddition of the simplest iminium ylide leading to 3- or 3,4-substituted pyrrolidines and 2,5-dihydropyrroles. *Chem. Pharm. Bull.* **1985**, *33*, 2762.

DOI: 10.1021/acsmedchemlett.9b00010
ACS Med. Chem. Lett. XXXX, XXX, XXX−XXX